

# A Theoretical Analysis of Efficiency Constrained Utility-Privacy Bi-Objective Optimization in Federated Learning

Hanlin Gu\*, Xinyuan Zhao\*, Gongxi Zhu, Yuxing Han, Yan Kang, Lixin Fan, *Member, IEEE*, and Qiang Yang, *Fellow, IEEE*

**Abstract**—Federated learning (FL) enables multiple clients to collaboratively learn a shared model without sharing their individual data. Concerns about utility, privacy, and training efficiency in FL have garnered significant research attention. Differential privacy has emerged as a prevalent technique in FL, safeguarding the privacy of individual user data while impacting utility and training efficiency. Within Differential Privacy Federated Learning (DPFL), previous studies have primarily focused on the utility-privacy trade-off, neglecting training efficiency, which is crucial for timely completion. Moreover, differential privacy achieves privacy by introducing controlled randomness (noise) on selected clients in each communication round. Previous work has mainly examined the impact of noise level ( $\sigma$ ) and communication rounds ( $T$ ) on the privacy-utility dynamic, overlooking other influential factors like the sample ratio ( $q$ , the proportion of selected clients). This paper systematically formulates an efficiency-constrained utility-privacy bi-objective optimization problem in DPFL, focusing on  $\sigma$ ,  $T$ , and  $q$ . We provide a comprehensive theoretical analysis, yielding analytical solutions for the Pareto front. Extensive empirical experiments verify the validity and efficacy of our analysis, offering valuable guidance for low-cost parameter design in DPFL.

**Index Terms**—trustworthy federated learning, multi-objective optimization, differential privacy

## I. INTRODUCTION

The escalating stringency of legal and regulatory parameters, exemplified by initiatives like GDPR<sup>1</sup> and HIPAA<sup>2</sup>, has imposed rigorous constraints on user privacy. This has led to a situation where the amalgamation of private data from distinct users or organizations for the purpose of training machine learning models is no longer allowed. Federated learning [1], [2] is a pioneering paradigm in machine learning that addresses the challenge of training models on decentralized data sources while respecting stringent privacy and security constraints. In federated learning, multiple participating entities or clients collaboratively train a shared machine learning model without directly sharing their raw data.

Recently, apart from traditional utility issue, privacy and efficiency issues in federated learning attract wide research at-

ention. In order to prevent privacy leakage from the exchanged information in FL, differential privacy has been proposed as an important privacy protection mechanism [3], [4], which is achieved by introducing noise into the exchanged gradients in the training process. In differential privacy federated learning (DPFL), there is a trade-off between utility and privacy as demonstrated in [5]–[7]. For instance, it was shown that attackers may infer training images at pixel level accuracy even random noise are added to exchanged gradients [8]–[12], but exceedingly large noise jeopardise learning reliability and lead to significant degradation of utility [5]–[7]. On the other hand, training efficiency which describes the global training time is also an important concern in the federated learning framework [13]–[15]. Ignoring the training efficiency may lead to exceedingly long training time outside an acceptable timeframe.

A series of work attempts to balance utility loss and privacy leakage in DPFL, but neglect the training efficiency. Specifically, these work provides different strategies to search for better parameters to look for optimal privacy-utility trade-off in DPFL. Some work [16], [17] aimed to minimize the utility loss while accounting for the resulting privacy leakage within the confines of a specified privacy budget ( $\epsilon_0$ ). Another line of work [5], [18] firstly trained the model until convergence with different noise extent. Subsequently, a comparison is drawn between resulting privacy leakages to identify the parameter settings that yield the least privacy leakage. However, the existing methods ignore the training efficiency in DPFL, which refers to the global training time (discussed in Sec. III-B in detail).

Moreover, in the process of searching optimal parameters, the traditional methods primarily concentrate on the influence of parameters as noise level ( $\sigma$ ) and communication rounds ( $T$ ), but ignore sample ratio ( $q$ ) as another important factor. Kang et al. [7] manipulate the noise level ( $\sigma$ ) to simultaneously enhance privacy, minimize utility and efficiency. Other works [5], [16]–[18] put forth different strategies to search for noise level ( $\sigma$ ) and communication rounds ( $T$ ) with aim of achieving optimal privacy-utility trade-off in DPFL. These methods neglects sample ratio (the ratio of participating clients in each round among all the  $K$  clients, denoted as  $q$ ), which has significant influence on both the utility loss [19], [20] and privacy leakage [4]. To look for the optimal trade-off by considering the influence of sample ratio ( $q$ ), a naive expansion of current methods as iterating over  $q$  suffers from really high

arXiv:2312.16554v2 [cs.LG] 29 Jan 2024

\* Hanlin Gu and Xinyuan Zhao contribute equally in this paper

† Yuxing Han is the corresponding author

This work was supported by the National Natural Science Foundation of China (NO.62206154) and Shenzhen Startup Funding (No. QD2023014C).

<sup>1</sup>GDPR is applicable as of May 25th, 2018 in all European member states to harmonize data privacy laws across Europe. <https://gdpr.eu/>

<sup>2</sup>HIPAA is a federal law of the USA created in 1996. It required the creation of national standards to protect sensitive patient health information from being disclosed without the patient's consent or knowledge

computation cost.

In this work, we formulate a constrained bi-objective optimization problem in Sect. III with aim of ensuring acceptable training efficiency and reducing optimal parameter searching computation cost. This formulation (Eq. 6) focuses on minimizing the privacy leakage and utility loss, and include an upper constraint of training efficiency to ensure acceptable training time in DPFL. It identifies the Pareto front encompassing the noise level ( $\sigma$ ), the communication rounds ( $T$ ) and sample ratio ( $q$ ). Moreover, we conduct theoretical analysis to offer insights into the interplay among various parameters in DPFL. Detailed theoretical findings can be found in Thm. 2 of Sect. IV. Notably, the Pareto optimal solutions for the constrained bi-objective optimization problem in DPFL adheres to the relationship  $k\sigma^2T = qK$  ( $K$  denotes the total number of clients;  $k$  is a constant), which serves as a powerful tool to help with low cost parameter design in DPFL discussed in Sec. V-D. Finally, experimental results in Sect. V also verify the theoretical analysis on Pareto optimal solutions<sup>3</sup> on MNIST dataset (with logistic regression and LeNet) and CIFAR-10 dataset (with ResNet-18). Our main contribution is summarized as following:

- We formulate the utility loss and privacy leakage with training efficiency upper constraint in differential privacy federated learning (DPFL) as constrained bi-objective optimization problem with respect to noise level ( $\sigma$ ), communication rounds ( $T$ ) and sample ratio ( $q$ ).
- We theoretically elucidate the analytical Pareto optimal solutions of the constrained bi-objective optimization problem in DPFL w.r.t.  $\sigma$ ,  $T$  and  $q$  under different participant numbers  $K$ .
- The experiments on MNIST and CIFAR-10 verify the correctness of our theoretical analysis of the constrained bi-objective optimization problem in DPFL. Moreover, it illustrates the theoretical analysis can guide clients to design the effective parameters in DPFL with much lower computation cost than traditional methods.

## II. RELATED WORK

### A. Federated Learning

With the aim of privacy protection and further improve the model performance, federated learning is proposed, where model is trained on distributed data with different privacy protection mechanisms. Clients update the model locally and periodically communicate with the central server to synchronize the model. Typically, federated learning deals with a single optimization problem where  $K$  clients collaboratively trains the model parameters  $w_{fed}$  [7].

$$\min_{w_{fed}} \epsilon_u(w_{fed}) \triangleq \sum_{k=1}^K \frac{n_k}{n} F_k(w_{fed}) \quad (1)$$

$$F_k(w_{fed}) = \mathbb{E}_{\xi \sim D_k} F(w_{fed}; \xi)$$

$n_k$  represents the size of dataset  $D_k$  kept within client  $k$  and  $n$  is the total size of dataset as  $n = \sum_{k=1}^K n_k$ . The local model

<sup>3</sup>The definition of Pareto optimal solutions are given in Part C: Bi-Objective Optimization, II. Related Work and Background

TABLE I  
TABLE OF NOTATION

Notation	Meaning
$\sigma$	noise level
$\sigma_{max}$	upper constraint of $\sigma$
$q$	sample ratio
$T$	communication rounds
$T_{max}$	maximum of communication round $t$
$E$	local training epochs within each round
$K$	total number of clients
$\epsilon_0$	privacy budget
$D_k$	private dataset of client $k$
$D_{test}$	test dataset
$w^t$	global model at round $t$
$\tilde{\Delta}w_k^t$	protected model gradients of client $k$ at round $t$
$w_k^{t,e}$	local model weight of client $k$ at round $t$ and local epochs $e$
$\Delta w_k^t$	model gradients of client $k$ at round $t$
$n_k^t$	Gaussian noise of client $k$ at round $t$
$c_{clip}$	clipping constant
$P_t$	participating clients at round $t$
$\eta$	learning rate
$B$	batch size
$(x, y)$	feature-label pair in dataset
$L_{ce}$	cross-entropy loss function
$\epsilon_p$	privacy leakage
$\epsilon_u$	utility loss
$\epsilon_e$	training efficiency
$\bar{\epsilon}_e$	upper constraint of training efficiency
$F_k$	inference model of client $k$

with the  $k^{th}$  client  $F_k$  is the expectation of the loss function regarding sampling from local dataset  $D_k$ .

The most well studied algorithm is federated average (FedAVG) and federated stochastic gradient descent (FedSGD) [1]. FedAVG parallel optimizes the local objective function by using stochastic gradient descent in each client and use trivial average to aggregate the model parameters at the server. FedSGD calculates the model update using randomly sampled local data, and upload the model update to central server. FedAVG and FedSGD is equivalent under the scenario that the number of local epochs  $E$  equals one.

### B. Differential Privacy

Differential privacy serves as a strong standard privacy guarantee, which is firstly introduced to protect single instance privacy in terms of adjacent databases [21]–[23]. Treating the image-label pair as a instance in database, the  $(\epsilon, \delta)$ -differential privacy is defined as follows.

**Definition 1** ( $(\epsilon, \delta)$ -differential privacy in [4]): A randomized mechanism  $\mathcal{M} : \mathcal{D} \rightarrow \mathcal{R}$  with domain  $\mathcal{D}$  and range  $\mathcal{R}$  satisfies  $(\epsilon, \delta)$ -differential privacy if for any two adjacent inputs  $d, d' \in \mathcal{D}$  and for any subset of outputs  $\mathcal{S} \subseteq \mathcal{R}$  it holds that

$$Pr[\mathcal{M}(d) \in \mathcal{S}] \leq e^\epsilon Pr[\mathcal{M}(d') \in \mathcal{S}] + \delta$$

where we say that two of these sets are adjacent if they differ in a single entry.

In deep learning scenario, a series of works under different assumptions are proposed to tighten the privacy leakage bound [24], [25] and moments accountant is introduced to quantitatively measure the privacy leakage [4].

**Theorem 1 (Thm. 1 of [4]):** There exists constant  $r$  and constant  $s$  so that given the sampling probability  $q = \frac{B}{N}$  ( $N$  is the number of training set) and the number of total rounds  $T$ , for any  $\epsilon < rq^2T$ , the differentially private SGD algorithm [4] is  $(\epsilon, \delta)$ -differentially private for any  $\delta > 0$  if we choose

$$\sigma \geq s \frac{q\sqrt{T\log(1/\delta)}}{\epsilon}$$

In federated learning, differential privacy also serves as a golden benchmark which people design different algorithms to achieve [26], [27].

### C. Multi-objective Optimization

In multi-objective optimization, the aim is to find a  $x$  in the decision space  $\mathcal{R}^d$  which can optimize a set of  $m$  objective functions as  $f_1(w), f_2(w), \dots, f_m(w)$  [28].

$$\min_{w \in \mathcal{R}^d} G(x) := \min(f_1(w), f_2(w), \dots, f_m(w))$$

In non-trivial case, all the objective functions cannot achieve their global optimum with the same  $x$ . The multi-objective optimization methods are used to deal with the contradictions and achieve different optimal trade-off among the objectives. From the point view of decision makers, the multi-objective optimization provides a set of optimal solutions based on different preference and requirements.

**Definition 2 (Pareto dominance in [29]):** For  $x_a, x_b \in \mathcal{R}^d$ , we say  $x_a$  dominates  $x_b$  if and only if  $f_i(x_a) < f_i(x_b)$  for at least one  $i \in [1, 2, \dots, n]$  and  $f_i(x_a) \leq f_i(x_b)$  for all  $i \in [1, 2, \dots, n]$ .

**Definition 3 (Pareto optimal solution in [29]):** We say  $x^*$  is a Pareto optimal solution if  $x^*$  dominates all other  $x' \in \mathcal{R}^d$ .

**Definition 4 (Pareto set and front in [29]):** Pareto set is the set of  $G(x_i)$   $i \in [1, 2, \dots, n]$ , where  $x_i$   $i \in [1, 2, \dots, n]$  is all the Pareto optimal solutions. Pareto front is the plot of Pareto set  $G(x_i)$   $i \in [1, 2, \dots, n]$  in the objective space.

Multi-objective optimization can be a challenging job in federated learning. People use different multi-objective optimization methods as evolutionary algorithms [30]–[33], Bayesian optimization [34]–[37], and gradient-based method [38]–[42] to deal with the multi-objective optimization problem in federated learning. Facing expensive black box scenarios as federated learning, evolutionary algorithms suffers from high computational cost especially facing expensive scenarios as federated learning. Bayesian optimization improves the computational efficiency, but its performance highly depends on the surrogate model and acquisition function. The gradient descent method improves the computational efficiency by finding the directions that simultaneously descend all the objective functions, but requires the gradient information of the objective function.

## III. MOO IN DPFL

In this section, we formulate the constrained bi-objective optimization in Differential Privacy Federated Learning (DPFL) by optimizing the privacy leakage and utility loss simultaneously with training efficiency constraint.

### A. Setting and Threat Model

We consider *horizontal federated learning* (HFL) in this paper, which involves  $K$  participating parties that each holds a private dataset  $D_k, k \in [K]$ . We assume the attacker to be *semi-honest*, i.e., it may launch *privacy attacks* on exchanged information to infer participants' private data. For instance, the semi-honest adversary may reconstruct the client's data via the exchanged model gradients [8], [9].

To mitigate the privacy leakage, each participant applies a protection mechanism to the model information that will be shared with the server. This paper focuses on the differential privacy [4], i.e., the local client adds noise on the model gradients. The training procedure involves at least three following steps in each round  $t$  (also see Algo. 1):

- 1) Each client  $k$  trains its local model using its private data set  $D_k$  for  $E$  local epochs, and obtains the local model  $w_k^{t,E}$  as in line 12-16 in Algo. 1.
- 2) In order to prevent semi-honest adversaries from inferring other clients' private information  $D_k$ , each client  $k$  clips model gradients  $\Delta w_k^t$  and adds Gaussian noise  $n_k^t$  as shown in line 17-18 of Algo. 1 The client sends protected model gradients  $\tilde{\Delta} w_k^t$  to the server as line 19 of Algo. 1.
- 3) The server aggregates  $\tilde{\Delta} w_k^t, k = 1, \dots, K$  by average in line 8 of Algo. 1. The global model  $w^{t+1}$  is updated to be  $w^{t+1} = w^t + \frac{1}{K} \sum_{i=1}^K \tilde{\Delta} w_k^t$ .  $w^{t+1} \leftarrow w^t + \frac{1}{|P_t|} \sum_{k \in |P_t|} \tilde{\Delta} w_k^t$ . Then the server distributes global model  $w^{t+1}$  to all clients.

### B. Privacy Leakage, Utility Loss, and Training Efficiency in DPFL

In this paper, we consider two objectives in the DPFL, i.e., the privacy leakage and utility loss, which is defined as following.

**Privacy Leakage.** We follow Thm. 1 of [4] and Thm. 3.2 of [43] to provide the definition of the differential privacy  $\epsilon_p$  leakage of local client in federated learning as:

$$\epsilon_p = C \frac{c_{clip} \sqrt{qT\log(1/\delta)}}{\sqrt{K}\sigma}, \quad (2)$$

where  $C$  is a constant,  $c_{clip}$  is the clipping constant in differential privacy,  $K$  is the total number of participants in federated learning and  $q$  is the the sample ratio representing the fraction of participating clients among all clients in each round.

According to Eq. (2), the privacy budget is influenced by three factors:  $q$ ,  $T$ , and  $\sigma$ . Specifically, the privacy leakage is positively related to  $q$  and  $T$  while negatively related to  $\sigma$ .

**Utility Loss.** The utility loss  $\epsilon_u$  of a federated learning system is defined as follows:

$$\epsilon_u = U(w_{fed}^O) - U(w_{fed}^D), \quad (3)$$

where  $U(w_{fed}^D)$  and  $U(w_{fed}^O)$  measure the utility of protected global model  $w_{fed}^D$  and unprotected global model  $w_{fed}^O$ , respectively. Moreover, the following Lemma 1 (Cor. 3.2.1 of [43]) provides the theoretical upper bound for Algo. 1.

**Lemma 1 (Adapted from Cor. 3.2.1 of [43]):** For Algo. 1, assume  $F_k(x)$  satisfies  $\|\nabla F_k(x) - \nabla F_k(y)\| \leq L\|x -$

**Algorithm 1 DP-FedSGD**( $T, q, \sigma$ ) (Algo. 3 of [43]): The  $K$  clients are indexed by  $k$ ,  $P_t$  is the set of participating clients in round  $t$ ;  $B$  is the local batch size,  $T$  is communication rounds,  $E$  is local training epochs;  $w^t$  is the global model at round  $t$ ,  $w_k^{t,e}$  is the local model of client  $k$  at round  $t$  and local epoch  $e$ ,  $\eta$  is the learning rate,  $c_{clip}$  is the clipping constant,  $\sigma$  is noise level,  $n_k^t$  follows  $\mathcal{N}(0, \sigma^2)$ ;  $D_{test}$  is the test dataset,  $(x_i, y_i)$  is the feature-label pair in  $D_{test}$ .

---

```

1: Server executes:
2: Randomly initialize  $w^0$ 
3: for  $t \in [0, 1, \dots, T - 1]$  do
4:   Distribute  $w_t$  to clients
5:   for Client  $k \in [P_t]$  in parallel do
6:      $\tilde{\Delta}w_k^t \leftarrow \mathbf{ClientUpdate}(k, w^t)$ 
7:   end for
8:   Aggregate model  $w^{t+1} \leftarrow w^t + \frac{1}{|P_t|} \sum_{k \in |P_t|} \tilde{\Delta}w_k^t$ 
9:   Evaluate test loss  $L_{ce}^t$  by cross-entropy loss function
      $L_{ce}(x_i, y_i; w^t), (x_i, y_i) \in D_{test}$ 
10: end for
11: Return test loss  $L_{ce}^t$  for all  $t, t \in [1, 2, \dots, T]$ 
12:
13: ClientUpdate( $k, w^t$ ): // Run on client  $k$ 
14: Initialize:  $w_k^{t,0} \leftarrow w^t$ 
15: for  $e \in [0, 1, \dots, E - 1]$  do
16:   Randomly sample batch  $b$  (size  $B$ ) in local training
     dataset  $D_k$ ;
17:   Compute gradient  $g_k^{t,e} = \nabla F_k(w_k^{t,e}; b)$ 
18:   Local update  $w_k^{t,e+1} \leftarrow w_k^{t,e} - \eta g_k^{t,e}$ 
19: end for
20: Compute the difference of model weights  $\Delta w_k^t = w_k^{t,E} -
     w_k^{t,0}$ 
21: Add noise  $\tilde{\Delta}w_k^t = \Delta w_k^t / \max(1, \frac{\|\Delta w_k^t\|^2}{c_{clip}}) + n_k^t$ 
22: Return and upload  $\tilde{\Delta}w_k^t$  to server.
```

---

$y||, \forall k, x, y, \min_x F(x) \geq F^*$ ,  $G$  is the bound on stochastic gradient,  $C_{clip}$  is the clipping constant with  $C_{clip} \geq \eta EG$ .  $\frac{\eta}{qK} \leq \eta$  as  $qK \geq 1$ .

By letting  $\eta \leq \min\{\frac{qK}{6EL(P-1)}, \frac{qK}{96E^2}, \frac{1}{\sqrt{60EL}}\}$ , we have

$$\frac{1}{T} \sum_{t=1}^T \mathbb{E}[\|\nabla F(x^t)\|^2] \leq \mathbf{O}\left(\frac{1}{\eta ET} + \eta^2 E^2 + \eta\right) + \mathbf{O}\left(\frac{\sigma^2}{\eta q K E}\right),$$

where  $T$  and  $E$  are communication rounds and local training epochs,  $\eta$  is learning rate,  $K$  is the total number of clients,  $q$  is sample ratio, and  $\sigma$  is the noise level in differential privacy (standard derivation of added noise).

Note that the upper bound of the utility loss goes up with the increase of  $\sigma$  and the decrease of  $q, T$ .

**Remark 1:**  $K$  and  $E$  are always pre-defined, which is explored in the experimental ablation study part V-C.  $c_{clip}$  is a given constant.

**Training Efficiency.** We use the system training time to describe the training efficiency in DPFL as follows:

$$\epsilon_e = c_t T \quad (4)$$

where  $T$  is the communication rounds and  $c_t$  is the per-round training time in DPFL, which is treated as a constant due to the nearly uniform training time per round.

### C. Constrained Bi-Objective Optimization in DPFL

Conventionally, existing work aims to minimize the utility loss given the privacy budget  $\epsilon_0$  [16], [17], which can be formulated as:

$$\min_{T, \sigma} \epsilon_u(T, \sigma), \text{ where } \epsilon_u(T, \sigma) = \sum_{k=1}^K p_k F_k(T, \sigma) \quad (5)$$

subject to  $\epsilon_p(T, \sigma) \leq \bar{\epsilon}_0$

where  $\epsilon_p, \epsilon_u$  and  $\bar{\epsilon}_0$  represent privacy leakage, utility loss and the upper constraint of privacy leakage respectively.

However, the existing work only focuses on utility loss and privacy leakage, but ignore the training efficiency. It means that existing work cannot ensure the acceptable training time in DPFL. Moreover, both the privacy leakage and utility loss are influenced by the training epoch ( $T$ ), noise level ( $\sigma$ ) and sample ratio ( $q$ ) illustrated in the former section. It means Eq. (5) is insufficient to obtain a complete Pareto optimal as it only considers the influence of  $\sigma$  and  $T$ . In this work, we reformulate the optimization problem as the following definition.

**Definition 5:** The utility loss and privacy leakage bi-objective optimization problem with training efficiency constraint w.r.t. noise level ( $\sigma$ ), communication round ( $T$ ), and sample ratio ( $q$ ) in DPFL is:

$$\min_{T, \sigma, q} (\epsilon_u(T, \sigma, q), \epsilon_p(T, \sigma, q)),$$

where  $\epsilon_u(T, \sigma, q) = \sum_{k=1}^K p_k F_k(T, \sigma, q)$

$$\epsilon_p(T, \sigma, q) = C \frac{c_{clip} \sqrt{q T \log(1/\delta)}}{\sqrt{K} \sigma} \quad (6)$$

subject to  $\epsilon_e(T, \sigma, q) \leq \bar{\epsilon}_e$ ,

where  $\epsilon_u$  represents utility loss,  $\epsilon_p$  represents the privacy leakage by Eq. (2),  $\epsilon_e$  represents the training efficiency by Eq. (4),  $p_k$  is the coefficient of  $F_k$  satisfying  $\sum_{k=1}^K p_k = 1$ ,  $\bar{\epsilon}_e$  is the upper constraint of training efficiency.

In the following sections, we provide the analysis the constrained bi-objective optimization problem both theoretically and experimentally. On one hand, we provide the theoretical analysis on the Pareto optimal solutions of Eq. (6) in Sec. IV. On the other hand, we solve the Eq. (6) by non-dominated sorting Algo. 2 in Sect. V-B to determine the Pareto optimal solutions. Moreover, the experimental results in Sect. V can validate the theoretical conclusion.

## IV. THEORETICAL ANALYSIS

In this section, we commence by simplifying the constrained bi-objective optimization problem through the utilization of an upper boundary for the utility loss in Sect. IV-A. Subsequently, we conduct a comprehensive theoretical investigation into the constrained bi-objective problem, culminating in the derivation of an analytical expression for the Pareto solution involving

---

**Algorithm 2** Multi-Objective Optimization in DPFL.
 

---

**Step1 Objective Function Calculation:**

**for** sample ratio  $q_i \in (0, 1]$  **do**  
   **for**  $\sigma_i \in (0, \sigma_{max}]$  **do**  
     Calculate test loss  $L_t$  for  $\forall T \in [T_{max}]$  by Algo. 1 as  
      $(L_1, L_2, \dots, L_{T_{max}}) = \text{DP-FedSGD}(T_{max}, \sigma_i, q_i)$   
     Calculate privacy leakage by Eq. (2) as  $\epsilon_p(T, \sigma_i, q_i) =$   
      $C \frac{c_{clip} \sqrt{q_i t \log(1/\delta)}}{\sqrt{K} \sigma_i} \forall T \in [T_{max}]$   
   **end for**  
**end for**

**Step2 Non-dominated Comparison:**

**for**  $(T_i, \sigma_i, q_i), \forall T_i, \sigma_i, q_i$  **do**  
   **if**  $(T_i, \sigma_i, q_i)$  Pareto dominates all  $(T_j, \sigma_j, q_j), \forall T_j, \sigma_j, q_j$   
   **then**  
      $(T_i, \sigma_i, q_i)$  is one of the Pareto optimal solutions  
   **end if**  
**end for**

**Step3 Output:**

Return the Pareto optimal solutions

---

three distinct parameters: communication rounds ( $T$ ), noise level ( $\sigma$ ), and sample ratio ( $q$ ) in Sect. IV-B. Our approach entails initially analysing the Pareto front and Pareto solution encompassing all three parameters with unconstrained  $q$  and  $\sigma$ . Moreover, with given  $q$  and constrained  $\sigma$ , we focus on  $T$  and  $\sigma$  and detailed analyze the Pareto solution in different cases.

### A. Simplified Formulation

We obtain a simplified version of the constrained bi-objective optimization formulation by using the differential privacy leakage  $\epsilon_p(T, \sigma, q)$ , upper bound of utility loss  $\epsilon_u(T, \sigma, q)$ , and training efficiency  $\epsilon_e$  illustrated in Sect. III-B.

$$\begin{aligned} & \min(f_1(T, \sigma, q), f_2(T, \sigma, q)) \\ & \text{where } f_1(T, \sigma, q) = \mathbf{O}\left(\frac{1}{\eta ET} + \eta^2 E^2 + \eta\right) + \mathbf{O}\left(\frac{\sigma^2}{\eta q K E}\right) \\ & \quad f_2(T, \sigma, q) = C \frac{c_{clip} \sqrt{q T \log(1/\delta)}}{\sqrt{K} \sigma} \\ & \text{subject to } f_3(T, \sigma, q) = c_t T \leq \bar{\epsilon}_e \end{aligned} \quad (7)$$

As the number of clients ( $K$ ), the local training epochs ( $E$ ), the learning rate ( $\eta$ ) and the clipping constant ( $c_{clip}$ ) are usually pre-decided in the real scenario, and the per-round training time  $c_t$  is approximately uniform each round, we keep  $K, E, c_{clip}$ , and  $c_t$  as constants.

Focusing on parameter  $\sigma, T$  and  $q$ , the constrained bi-objective formulation can be further simplified as follows

according to Lemma 2.

$$\begin{aligned} & \min(f_1(T, \sigma, q), f_2(T, \sigma, q)) \\ & \text{where } f_1(T, \sigma, q) = \frac{1}{T} + k \frac{\sigma^2}{qK}, \quad k \text{ is constant} \\ & \quad f_2(T, \sigma, q) = \frac{\sqrt{qT}}{\sigma} \\ & \text{subject to } f_3(T, \sigma, q) = c_t T \leq \bar{\epsilon}_e \end{aligned} \quad (8)$$

With aim of simplifying the optimization objective functions, we provide the following lemma.

**Lemma 2:** The Pareto optimal solutions of Eq. (9) and Eq. (10) are equivalent, where constants  $a_1, a_2 \in \mathbf{R}^+$  and constants  $m_1, m_2 \in \mathbf{R}$ .

$$\begin{cases} f_1(x) = a_1 \times h_1(x) + m_1 \\ f_2(x) = a_2 \times h_2(x) + m_2 \end{cases} \quad (9)$$

$$\begin{cases} f'_1(x) = h_1(x) \\ f'_2(x) = h_2(x) \end{cases} \quad (10)$$

**Proof 1:** Suppose that  $x_0$  is a Pareto optimal solution of Eq. (9). We have Eq. (11) according to the definition of Pareto optimal solution.

$$\begin{aligned} & \forall x_i \neq x_0, \forall j \in [1, 2], f_j(x_0) \leq f_j(x_i) \\ & \quad \exists j \in [1, 2], f_j(x_0) < f_j(x_i) \end{aligned} \quad (11)$$

$$\begin{aligned} & \iff \forall x_i \neq x_0, \\ & \quad \forall j \in [1, 2], a_j h_j(x_0) + m_j \leq a_j h_j(x_i) + m_j \\ & \quad \exists j \in [1, 2], a_j h_j(x_0) + m_j < a_j h_j(x_i) + m_j \end{aligned} \quad (12)$$

$$\begin{aligned} & \iff \forall x_i \neq x_0, \forall j \in [1, 2], h_j(x_0) \leq h_j(x_i) \\ & \quad \exists j \in [1, 2], h_j(x_0) < h_j(x_i) \end{aligned} \quad (13)$$

$$\begin{aligned} & \iff \forall x_i \neq x_0, \forall j \in [1, 2], f'_j(x_0) \leq f'_j(x_i) \\ & \quad \exists j \in [1, 2], f'_j(x_0) < f'_j(x_i) \end{aligned} \quad (14)$$

It has been proved that  $x_0$  is still a Pareto optimal solution of optimization problem Eq. (10). The Pareto optimal solutions of Eq. (9) and Eq. (10) are equivalent.

### B. Pareto Optimal Solutions

In this section, we derive the analytical Pareto optimal solutions w.r.t  $T, \sigma$  and  $q$  in Thm. 2 and the analytical Pareto optimal solutions with pre-defined  $q$  under different constraint cases in Cor. 3.

**Theorem 2: (Analytical Solutions w.r.t.  $q, T, \sigma$  with unconstrained  $\sigma$  and  $q$ )** Assuming  $\sigma \in [0, +\infty)$  and  $q \in (0, 1]$ , we have the Pareto optimal solutions for Eq. (8) as follows.

$$k\sigma^2 T = qK, \quad (15)$$

where  $k, t_c$  is constant and  $T \in [1, \dots, \lfloor \frac{\bar{\epsilon}_e}{t_c} \rfloor]$ .

**Proof 2:** Set  $X = \frac{1}{T} + \frac{k}{K} \frac{\sigma^2}{q}$  with constant  $k$ . The bi-objective optimization objective functions  $f_1$  and  $f_2$  in Eq. (8) is converted to the following form:

$$\begin{aligned} & f_1(X, \sigma, q) = X, \\ & \quad f_2(X, \sigma, q) = \sqrt{\frac{q}{\sigma^2(X - k \frac{\sigma^2}{qK})}}, \end{aligned} \quad (16)$$

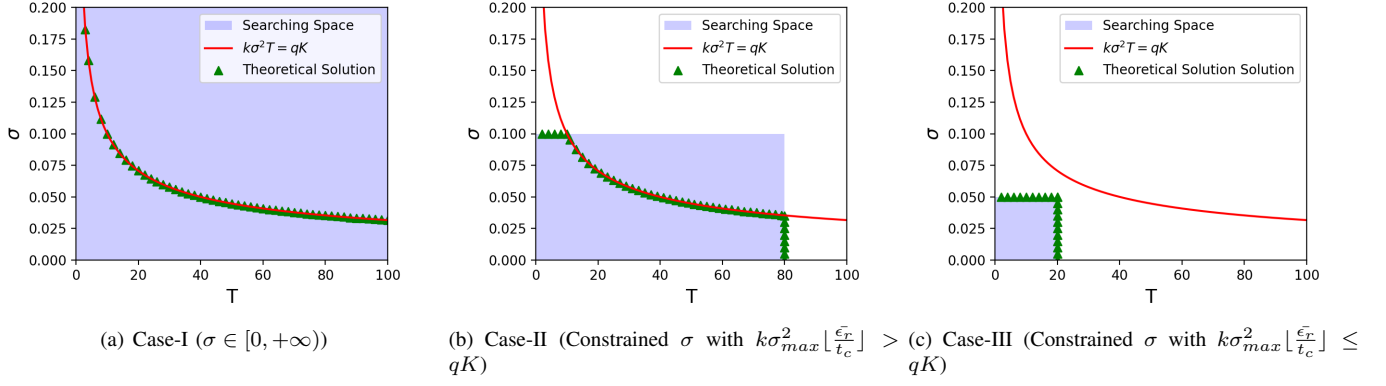


Fig. 1. Theoretical Pareto Optimal Solutions.  $T$  is on x-axis and  $\sigma$  is on y-axis. The blue area is the decision space with constraint. The red line represents the inverse proportional relationship between  $\sigma^2$  and  $T$ , and the green triangle represents the analytical solution.

where  $X \in (0, +\infty)$ ,  $q \in (0, +\infty)$ ,  $\sigma \in (0, +\infty)$ .

For a specific  $X$ ,  $f_2$  reaches minimum  $\frac{2\sqrt{k}}{\sqrt{KX}}$  when  $\frac{\sigma^2}{q} = \frac{KX}{2k}$  according to inequality of arithmetic means. Specifically,

$$\begin{aligned} f_2(\sigma^2, q|X) &= \sqrt{\frac{1}{\frac{\sigma^2}{q}(X - \frac{k}{K}\frac{\sigma^2}{q})}} \\ &\geq f_2\left(\frac{\sigma^2}{q} = \frac{KX}{2k} | X\right) = \frac{2\sqrt{k}}{\sqrt{KX}}. \end{aligned} \quad (17)$$

Therefore, given  $X$ ,  $(X, \frac{2\sqrt{k}}{\sqrt{KX}})$  Pareto dominates the set  $\{(X, \sqrt{\frac{q}{\sigma^2(X - \frac{k}{K}\frac{\sigma^2}{q})}}) | \frac{\sigma^2}{q} \neq \frac{KX}{2k}, \forall \sigma, q\}$ . As a result, the Pareto set of Eq. (8) must be a subset of  $\{(X, \frac{2\sqrt{k}}{\sqrt{KX}}), \forall X\} \triangleq S$ . Since each points in  $S$  non-dominates each other, the set  $S$  is the Pareto set of Eq. (8).

Moreover, by substituting  $X$  via Eq.  $\frac{\sigma^2}{q} = \frac{KX}{2k}$ , we have proven that the Pareto optimal solutions follows:

$$\begin{aligned} \frac{\sigma^2}{q} = \frac{KX}{2k} &\iff \frac{\sigma^2}{q} = \frac{K(\frac{1}{T} + k\frac{\sigma^2}{qK})}{2k} \\ &\iff k\sigma^2 T = qK. \end{aligned} \quad (18)$$

where  $k, t_c$  is constant and  $T \in [1, \dots, \lfloor \frac{\epsilon_r}{t_c} \rfloor]$ .

We have finished the proof.

**Remark 2:** In Proof 2, the bi-objective optimization objective functions as Eq. (16) can be written w.r.t.  $\frac{\sigma^2}{q}$  and  $T$  as follows:

$$\begin{aligned} f_1(X, \frac{\sigma^2}{q}) &= X, \\ f_2(X, \frac{\sigma^2}{q}) &= \sqrt{\frac{1}{\frac{\sigma^2}{q}(X - \frac{k}{K}\frac{\sigma^2}{q})}}. \end{aligned} \quad (19)$$

where  $X = \frac{1}{T} + \frac{k}{K}\frac{\sigma^2}{q}$ .

The Pareto optimal solutions as Eq. (18) can also be written w.r.t.  $\frac{\sigma^2}{q}$  and  $T$  as follows:

$$\frac{\sigma^2}{q} T = \frac{K}{k}. \quad (20)$$

Therefore, the fraction  $\frac{\sigma^2}{q}$  can be regarded as a single parameter in Proof 2. Based on that, keeping one of  $\sigma, q$  as a

constant and iterating over the other one can still achieve the whole Pareto front with unconstrained  $\sigma$  and  $q$ .

In the real scenario, the sample ratio ( $q$ ) is usually decided by the server and distributed to the clients. Based on this common setting, we keep sample ratio ( $q$ ) as a constant and further provides the analytical solutions w.r.t.  $\sigma$  and  $T$  as Theorem 3 under different cases. We also demonstrate the different cases analytical solutions in Fig. 1.

**Theorem 3:** With a pre-defined sample ratio ( $q$ ), the Pareto solution for Eq. (8) is as follows in the three cases:

- Case-I (Unconstrained  $\sigma$ ). Assuming  $\sigma \in [0, +\infty)$ , we have the Pareto optimal solution as follows:

$$k\sigma^2 T = qK, \quad k \text{ is constant}, \quad (21)$$

where  $k, t_c, q$  is constant and  $T \in [1, \dots, \lfloor \frac{\epsilon_r}{t_c} \rfloor]$ .

- Case-II (Constrained  $\sigma$  with  $k\sigma_{max}^2 \lfloor \frac{\epsilon_r}{t_c} \rfloor > qK$ ). Assuming  $\sigma \in [0, \sigma_{max}]$  and  $k\sigma_{max}^2 \lfloor \frac{\epsilon_r}{t_c} \rfloor > qK$ , we have the Pareto optimal solutions as follows:

$$\begin{cases} \sigma = \sigma_{max} & \text{when } T \in \{1, \dots, \lfloor \frac{qK}{k\sigma_{max}^2} \rfloor\} \\ \sigma = \sqrt{\frac{qK}{kT}} & \text{when } T \in \{\lfloor \frac{qK}{k\sigma_{max}^2} \rfloor, \dots, \lfloor \frac{\epsilon_r}{t_c} \rfloor - 1\} \\ \sigma = [0, \sqrt{\frac{qK}{k\lfloor \frac{\epsilon_r}{t_c} \rfloor}}] & \text{when } T = \lfloor \frac{\epsilon_r}{t_c} \rfloor. \end{cases} \quad (22)$$

- Case-III (Constrained  $\sigma$  with  $k\sigma_{max}^2 \lfloor \frac{\epsilon_r}{t_c} \rfloor \leq qK$ ). Assuming  $\sigma \in [0, \sigma_{max}]$  and  $k\sigma_{max}^2 \lfloor \frac{\epsilon_r}{t_c} \rfloor \leq qK$ , the Pareto optimal solutions are as follows.

$$\begin{cases} \sigma = \sigma_{max} & \text{when } T \in \{1, 2, \dots, \lfloor \frac{\epsilon_r}{t_c} \rfloor - 1\} \\ \sigma = [0, \sigma_{max}] & \text{when } T = \lfloor \frac{\epsilon_r}{t_c} \rfloor \end{cases} \quad (23)$$

**Proof 3:** Set  $X = \frac{1}{T} + \frac{k}{K}\frac{\sigma^2}{q}$  with constant  $k$  and  $q$ . The bi-objective optimization objective functions  $f_1$  and  $f_2$  in Eq. (8) is converted to the following form Eq. (24) and Eq. (25):

$$f_1(X, \sigma) = X$$

$$f_2(X, \sigma) = \sqrt{\frac{q}{\sigma^2(X - k\frac{\sigma^2}{qK})}} \quad (24)$$

$$f_1(X, T) = X$$

$$f_2(X, T) = \sqrt{\frac{kT^2}{K(XT - 1)}} \quad (25)$$

Set  $T_{max} = \lfloor \frac{\bar{c}_r}{t_c} \rfloor$ . The constraint as  $f_3(T, \sigma, q) = c_t T \leq \bar{c}_e$  in Eq. 8 can be converted to the form:

$$f_3(T, \sigma, q) = c_t T \leq \bar{c}_e, T \in \mathbb{Z}^+ \iff T \leq \frac{\bar{c}_e}{c_t}, T \in \mathbb{Z}^+$$

$$\iff T \in [1, 2, \dots, T_{max}]. \quad (26)$$

**Case-I (Unconstrained  $\sigma$ )** In Case-I, we have  $\sigma \in [0, +\infty)$ , given  $q$ , and  $T \in [1, 2, \dots, T_{max}]$ . For a specific  $X$ ,  $f_2$  reaches minimum value  $\frac{2\sqrt{k}}{\sqrt{KX}}$  when  $\sigma^2 = \frac{qKX}{2k}$  according to inequality of arithmetic means. Specifically,

$$f_2(\sigma^2|X) = \sqrt{\frac{q}{\sigma^2(X - k\frac{\sigma^2}{qK})}}$$

$$\geq f_2(\sigma^2 = \frac{qKX}{2k}|X) = \frac{2\sqrt{k}}{\sqrt{KX}}. \quad (27)$$

Therefore, given  $X$ ,  $(X, \frac{2\sqrt{k}}{\sqrt{KX}})$  Pareto dominates the set  $\{(X, \sqrt{\frac{q}{\sigma^2(X - k\sigma^2/(qK))}})|\sigma^2 \neq \frac{qKX}{2k}, \forall \sigma\}$ . As a result, the Pareto set of Eq. (8) must be a subset of  $\{(X, \frac{2\sqrt{k}}{\sqrt{KX}}), \forall X\} \triangleq S$ . Since each points in  $S$  non-dominates each other, the set  $S$  is the Pareto set of Eq. (8).

Moreover, by substituting  $X$  via Eq.  $\sigma^2 = \frac{qKX}{2k}$ , we have proven that the Pareto solution follows:

$$\sigma^2 = \frac{qKX}{2k} \iff \sigma^2 = \frac{qK(\frac{1}{T} + k\frac{\sigma^2}{qK})}{2k} \quad (28)$$

$$\iff k\sigma^2 T = qK.$$

**Case-II (Constrained  $\sigma$  with  $k\sigma_{max}^2 \lfloor \frac{\bar{c}_r}{t_c} \rfloor > qK$ )** As  $T_{max} = \lfloor \frac{\bar{c}_r}{t_c} \rfloor$ , we have  $T \in [1, \dots, T_{max}]$  and  $k\sigma_{max}^2 T_{max} > qK$  with  $\sigma \in [0, \sigma_{max}]$  and given  $q$ . We separate the value of  $X$  into three parts.

- Given  $X \in [\frac{1}{T_{max}}, \frac{2}{T_{max}})$ , we have  $\frac{X}{2} < \frac{1}{T_{max}} \leq \frac{1}{T}$ ,  $\forall T \in [1, 2, \dots, T_{max}]$ .  $f_2$  monotonically decrease when  $T < \frac{2}{X}$ .

$$f_2(T|X) = \sqrt{\frac{kT^2}{K(XT - 1)}} \geq f_2(T = T_{max}|X)$$

$$= \sqrt{\frac{kT_{max}^2}{K(XT_{max} - 1)}} \quad (29)$$

Therefore, given  $X \in [\frac{1}{T_{max}}, \frac{2}{T_{max}})$ ,  $(X, \sqrt{\frac{kT_{max}^2}{K(XT_{max} - 1)}})$  Pareto dominates the set  $\{(X, \sqrt{\frac{kT^2}{K(XT - 1)}})|T \neq T_{max}, \forall T\} \triangleq S_1$ .

- Given  $X \in [\frac{2}{T_{max}}, \frac{2k\sigma_{max}^2}{q}]$ ,  $f_2$  reaches minimum  $\frac{2\sqrt{k}}{\sqrt{KX}}$  when  $\sigma^2 = \frac{qKX}{2k}$  according to inequality of arithmetic means.

$$f_2(\sigma^2|X) = \sqrt{\frac{q}{\sigma^2(X - k\frac{\sigma^2}{qK})}}$$

$$\geq f_2(\sigma^2 = \frac{qKX}{2k}|X) = \frac{2\sqrt{k}}{\sqrt{KX}}. \quad (30)$$

Therefore, given  $X \in [\frac{2}{T_{max}}, \frac{2k\sigma_{max}^2}{q}]$ ,  $(X, \frac{2\sqrt{k}}{\sqrt{KX}})$  Pareto dominates the set  $\{(X, \sqrt{\frac{q}{\sigma^2(X - k\sigma^2/(qK))}})|\sigma^2 \neq \frac{qKX}{2k}, \forall \sigma\} \triangleq S_2$ .

- Given  $X \in (\frac{2k\sigma_{max}^2}{qK}, 1 + \frac{k\sigma_{max}^2}{qK})$ , we have  $\frac{qKX}{2k} > \sigma_{max}^2 \geq \sigma^2$ .  $f_2$  monotonically decrease when  $\sigma^2 < \frac{qKX}{2k}$

$$f_2(\sigma^2|X) = \sqrt{\frac{q}{\sigma^2(X - k\sigma^2/(qK))}} \geq f_2(\sigma = \sigma_{max}|X)$$

$$= \sqrt{\frac{q}{\sigma_{max}^2(X - k\sigma_{max}^2/(qK))}} \quad (31)$$

Therefore, given  $X \in (\frac{2k\sigma_{max}^2}{qK}, 1 + \frac{k\sigma_{max}^2}{qK})$ ,  $(X, \sqrt{\frac{q}{\sigma_{max}^2(X - k\sigma_{max}^2/(qK))}})$  Pareto dominates the set  $\{(X, \sqrt{\frac{q}{\sigma^2(X - k\sigma^2/(qK))}})|\sigma^2 \neq \sigma_{max}, \forall \sigma\} \triangleq S_3$ .

As a result, the Pareto set of Eq. (8) must be a subset of  $S_1 \cup S_2 \cup S_3 \triangleq S$ . Since each points in  $S$  non-dominates each other, the set  $S$  is the Pareto set of Eq. (8). We derive the Pareto solution set based on the Pareto front in the following.

- For  $X \in [\frac{1}{T_{max}}, \frac{2}{T_{max}})$ , it reaches Pareto front when  $T = T_{max}$ . We have the following Pareto solutions.

$$\forall \sigma \in [0, \sqrt{\frac{qK}{kT_{max}}}], T = T_{max} \quad (32)$$

- For  $X \in [\frac{2}{T_{max}}, \frac{2k\sigma_{max}^2}{qK}]$ , it reaches Pareto front when  $\sigma = \sqrt{\frac{qKX}{2k}}$ . As  $\sigma = \sqrt{\frac{qKX}{2k}}$  is equivalent to  $\sigma^2 T = \frac{qK}{k}$ , we have the following Pareto solutions.

$$\sigma = \sqrt{\frac{qK}{kT}} \text{ when } T \in \{ \lfloor \frac{qK}{k\sigma_{max}^2} \rfloor, \dots, T_{max} - 1 \} \quad (33)$$

- For  $X \in (\frac{2k\sigma_{max}^2}{qK}, 1 + \frac{k\sigma_{max}^2}{qK})$ , it reaches Pareto front when  $\sigma = \sigma_{max}$ . We have the following Pareto solutions.

$$\sigma = \sigma_{max} \text{ when } T \in \{1, \dots, \lfloor \frac{qK}{k\sigma_{max}^2} \rfloor\} \quad (34)$$

As  $T_{max} = \lfloor \frac{\bar{c}_r}{t_c} \rfloor$ , we have done the proof of Case-II.

**Case-III (Constrained  $\sigma$  with  $k\sigma_{max}^2 \lfloor \frac{\bar{c}_r}{t_c} \rfloor \leq qK$ )** As  $T_{max} = \lfloor \frac{\bar{c}_r}{t_c} \rfloor$ , we have  $T \in [1, \dots, T_{max}]$  and  $k\sigma_{max}^2 T_{max} \leq qK$  with  $\sigma \in [0, \sigma_{max}]$  and given  $q$ . We separate the value of  $X$  into two parts.

- Given  $X \in [\frac{1}{T_{max}}, \frac{1}{T_{max}} + \frac{k\sigma_{max}^2}{qK})$ , we have

$$X < \frac{1}{T_{max}} + \frac{k\sigma_{max}^2}{qK} < \frac{1}{T_{max}} + \frac{k}{qK} \frac{qK}{kT_{max}}, \quad (35)$$

which means  $T \leq T_{max} < \frac{2}{X} \cdot f_2$  monotonically decrease when  $T < \frac{2}{X}$ .

$$f_2(T|X) = \sqrt{\frac{kT^2}{K(XT-1)}} \geq f_2(T = T_{max}|X) = \sqrt{\frac{kT_{max}^2}{K(XT_{max}-1)}} \quad (36)$$

Therefore, given  $X \in [\frac{1}{T_{max}}, \frac{2}{T_{max}})$ ,  $(X, \sqrt{\frac{kT_{max}^2}{K(XT_{max}-1)}})$

Pareto dominates the set  $\{(X, \sqrt{\frac{kT^2}{K(XT-1)}}) | T \neq T_{max}, \forall T\} \triangleq S_1$ .

- Given  $X \in [\frac{1}{T_{max}} + \frac{k\sigma_{max}^2}{qK}, 1 + \frac{k\sigma_{max}^2}{qK}]$ , we have

$$X \geq \frac{1}{T_{max}} + \frac{k\sigma_{max}^2}{qK} > \frac{k\sigma_{max}^2}{qK} + \frac{k\sigma_{max}^2}{qK}, \quad (37)$$

which means  $\sigma^2 < \frac{qKX}{2k}$ .  $f_2$  monotonically decrease when  $\sigma^2 < \frac{qKX}{2k}$

$$f_2(\sigma^2|X) = \sqrt{\frac{q}{\sigma^2(X - k\sigma^2/(qK))}} \geq f_2(\sigma = \sigma_{max}|X) = \sqrt{\frac{q}{\sigma_{max}^2(X - k\sigma_{max}^2/(qK))}} \quad (38)$$

Therefore, given  $X \in [\frac{1}{T_{max}} + \frac{k\sigma_{max}^2}{qK}, 1 + \frac{k\sigma_{max}^2}{qK}]$ ,

$(X, \sqrt{\frac{q}{\sigma_{max}^2(X - k\sigma_{max}^2/(qK))}})$  Pareto dominates the set  $\{(X, \sqrt{\frac{q}{\sigma^2(X - k\sigma^2/(qK))}}) | \sigma^2 \neq \sigma_{max}, \forall \sigma\} \triangleq S_2$ .

As a result, the Pareto set of Eq. (8) must be a subset of  $S_1 \cup S_2 \triangleq S$ . Since each points in  $S$  non-dominates each other, the set  $S$  is the Pareto set of Eq. (8). We derive the Pareto solution set based on the Pareto front in the following.

- For  $X \in [\frac{1}{T_{max}}, \frac{1}{T_{max}} + \frac{k\sigma_{max}^2}{qK}]$ , it reaches Pareto front when  $T = T_{max}$ . We have the following Pareto solutions.

$$\forall \sigma \in [0, \sigma_{max}], T = T_{max} \quad (39)$$

- For  $X \in [\frac{1}{T_{max}} + \frac{k\sigma_{max}^2}{qK}, 1 + \frac{k\sigma_{max}^2}{qK}]$ , it reaches Pareto front when  $\sigma = \sigma_{max}$ . We have the following Pareto solutions.

$$\sigma = \sigma_{max}, \text{ when } T \in \{1, 2, \dots, T_{max} - 1\} \quad (40)$$

As  $T_{max} = \lfloor \frac{\epsilon_x}{t_c} \rfloor$ , we have done the proof of Case-III.

We have done the proof of the relationship between Pareto optimal  $\sigma$ ,  $T$ , and  $q$  of all the three cases. The theoretical analysis provides a theoretical guarantee for guiding optimal parameter design with low cost in DPFL.

## V. EXPERIMENT

In this section, we use experiments to verify our theoretical analysis. Firstly, we display the Pareto solutions of the efficiency constrained utility-privacy bi-objective optimization problem in DPFL regarding noise level ( $\sigma$ ), communication rounds ( $T$ ), and sample ratio ( $q$ ) in Sec.V-B. Secondly, we further investigate the influence of the total number of participating clients ( $K$ ) and the local training epochs ( $E$ ) on Pareto solutions in Sec.V-C. Finally, we demonstrate the process of low cost parameter design guiding by Thm. 2 and Cor. 3 in Sec.V-D.

### A. Experimental Setup

We implement both LR (logistic regression) and LeNet [44] on the MNIST [45] dataset, and employ ResNet-18 [46] on the CIFAR10 [47] dataset to verify our theoretical analysis. The MNIST dataset includes 60000 training samples and 10000 testing samples. The CIFAR-10 dataset includes 50000 training samples and 10000 testing samples. The samples are identically divided to  $K$  parts and kept locally within each client.

The communication rounds  $T_{max}$  is set to be 200. For LR model, the range of  $\sigma$  is set to be within  $[0.010, 0.150]$ . For LeNet model, the range of  $\sigma$  is set to be within  $[0.010, 0.050]$ . For ResNet-18 model, the range of  $\sigma$  is set to be within  $[0.0005, 0.0200]$ . Having batch size  $B = 64$ , we use stochastic gradient descent optimizer with learning rate  $\eta = 0.01$  and momentum as 0.09. To better estimate the test loss, we use multiple random seeds (30 for LR, 50 for LeNet, 36 for ResNet-18) and take average among the test loss of different seeds for different given  $\sigma$ ,  $T$ , and  $q$ .

### B. Pareto Solution in DPFL

We present the Pareto solutions from both theoretical and experimental perspectives, as depicted in Fig. 2. In our approach, we employ non-dominated sorting, as outlined in Algo. 2, to identify the experimental Pareto solution represented by the black points. We then compare this experimental solution on MNIST and CIFAR-10 with the theoretical solution derived in Thm. 2, illustrated separately in Fig. 2(a), Fig. 2(b), and 2(c). Notably, Fig. 2 reveals a strong alignment between the experimental and theoretical Pareto solutions, signifying the accuracy of our theoretical model.

Furthermore, to provide additional confirmation of the Pareto solutions derived in Cor. 3, we present a comparison of the theoretical and experimental Pareto solutions for different cases with a fixed  $q$ , as illustrated in Fig. 3.

Across all the three cases mentioned in Thm. 2, the Pareto solutions obtained through Algo. 2 (depicted as black points) align closely with the theoretical solutions (represented by green surface) established in Cor. 3. This consistency serves as strong evidence of the validity and reliability of our analytical model in predicting the Pareto front under various conditions.

### C. Ablation Study on $K, E$

In this subsection, we investigate the impact of local epochs ( $E$ ) and the number of clients ( $K$ ) on the Pareto solutions with a fixed sample ratio ( $q$ ), as discussed in Cor. 3. Our analysis yields the following three key conclusions:

- **Local Epochs ( $E$ ) Exhibit Minimal Influence:** We find that the local epochs ( $E$ ) have a negligible impact on the Pareto solutions. This observation is consistent across cases where  $E$  is set to different values, such as  $E = 5, 10, 20$ , as demonstrated in Fig. 4. This similarity in Pareto solutions indicates that the choice of  $E$  does not significantly alter the parameters for achieving the optimal trade-off between privacy and utility.
- **Number of Clients ( $K$ ) Affects Pareto Solution directly:** We observe that changes in the experimental



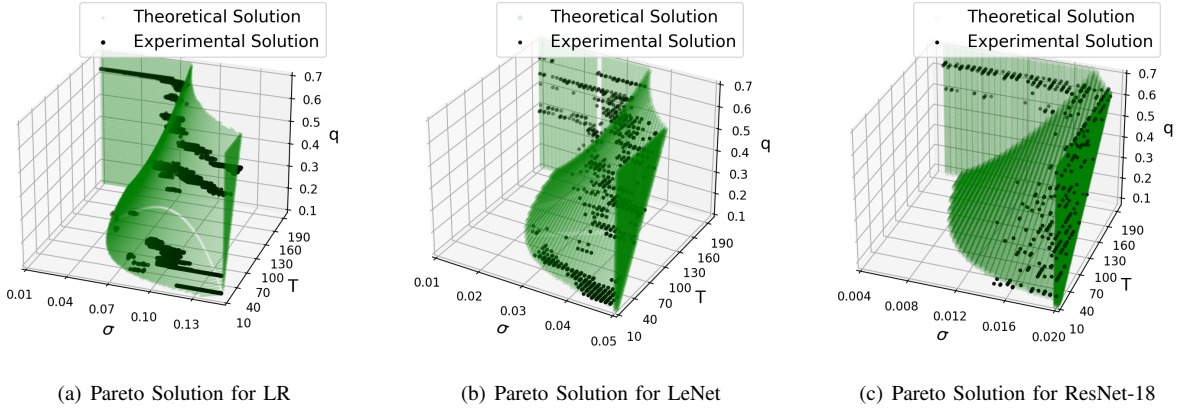


Fig. 2. **Pareto Front and Pareto Solution for LeNet and LR with respect to  $\sigma$ ,  $T$ , and  $q$ .** With total 40 clients and 20 local epochs in LR model, Fig. 2(a) compares the theoretical solutions with the experimental solutions. The green dots show the theoretical solutions with constant  $k = 22$  which means  $22\sigma^2T = 40q$ . The black dots show the experimental solutions by Algo. 2 with  $q \in [0.125, 0.2, 0.375, 0.4, 0.45, 0.55, 0.625]$ . With total 40 clients and 20 local epochs in LeNet model, Fig. 2(b) compares the theoretical solutions with the experimental solutions. The green dots show the theoretical solutions with constant  $k = 110$  which means  $110\sigma^2T = 40q$ . The black dots show the experimental solutions by Algo. 2 with  $q \in [0.125, 0.2, 0.25, 0.3, 0.375, 0.4, 0.5, 0.55, 0.625]$ . With total 40 clients and 20 local epochs in ResNet-18 model, Fig. 2(c) compares the theoretical solutions with the experimental solutions. The green dots show the theoretical solutions with constant  $k = 440$  which means  $440\sigma^2T = 40q$ . The black dots show the experimental solutions by Algo. 2 with  $q \in [0.125, 0.2, 0.25, 0.3, 0.375, 0.5, 0.625]$ .

Pareto solution concerning  $\sigma$  and  $T$  (as indicated by the black points in Figure 5) exhibit a direct relationship with the number of participating clients, denoted as  $K$ . Specifically, the relationship between  $\sigma$  and  $T$  follows the equation  $k\sigma^2T = qK$ , which is represented by the green line in Figure 5. This relationship implies that as the number of clients increases, the values of  $\sigma$  and  $T$  must adjust accordingly to maintain consistent Pareto solutions.

These findings provide valuable insights into the factors that influence the Pareto solutions in the context of federated learning with differential privacy, enabling practitioners to make informed decisions when designing privacy-preserving algorithms.

#### D. Demonstration of low cost Parameter Design

In the real scenario, due to the privacy preserved limitation and training efficiency constraint, it is not realistic to do a large number of experiments to search for the best parameters as communication rounds ( $T$ ), noise level ( $\sigma$ ) and sample ratio ( $q$ ). In other words, making sure the privacy leakage and utility loss reach the Pareto front with acceptable training efficiency in DPFL can be a challenging job. To deal with the challenge, the theoretical analysis (Thm. 2) can serve as an important guidance for the low cost parameter design of DPFL framework. Specifically, the parameter design process is structured into two distinct stages:

- 1) In the first step, using a small portion of a public dataset and keeping the sample ratio fixed at  $q_0$ , given the acceptable training efficiency constraint, along with the total number of clients set to  $K_0$ , clients undertake pre-experiments, following the procedure outlined in Algo. 2. These experiments aim to identify the Pareto optimal solutions corresponding to the noise level ( $\sigma$ ) and the global epoch ( $T$ ), represented as the black points in Fig. 6(a) and 6(d). Subsequently, clients extrapolate the behavior of these black points by utilizing the relationship

$k\sigma^2T = q_0K_0$  (depicted as the red line in Fig. 6(a) and 6(d)). This extrapolation further enables the estimation of the constant  $k^4$ .

- 2) In the second step, the server uniformly distributes the common sample ratio  $q_r$  and global training epoch ( $T_r$ ) to all participating clients. Each client then calculates their respective noise level, denoted as  $\sigma_r$ , based on the formula  $\sigma_r = \sqrt{\frac{q_r K}{k T_r}}$ .

Take two examples for LeNet and LR model, let the number of clients ( $K_r$ ) and sample ratio ( $q_r$ ) be 40 and 0.5 respectively. For the public dataset, we randomly sample 10% of original MNIST dataset. With  $q_0 = 1.0$  and  $K_0 = 10$ , the constant  $k$  is estimated to be 2.5 and 15.0 for LR and LeNet model separately as illustrated in Fig. 6(a) and 6(d). Then, to validate the correctness of the estimated constant  $k$ , we compare the theoretical solutions and experimental solutions of LR and LeNet model shown in Fig. 6(b) and 6(e) respectively. We derive the theoretical solutions by using the consistent constant  $k$  and represent the solutions by green points. The black points represent the experimental solutions, which are obtained via Algo. 2 using all MINTS data. Figure 6(c) and 6(f) demonstrate that these black points align with the theoretical Pareto front obtained using the estimated values of  $k$ .

We compare the computation cost (the time of guiding parameter design and the time of achieving Pareto set) of our method with the existing two types of methods. The first method named as **Training with Budget** [16], [17] is to minimize the utility loss when the privacy leakage is below the specified privacy budget. The second method named as **Training until Convergences** [5], [18] is to minimize the utility loss until the model convergence with different noise level and identify the optimal noise level with the least privacy

<sup>4</sup>It's important to note that this constant  $k$  remains consistent whether considering two parameters,  $\sigma$  and  $T$ , or three parameters, namely,  $q$ ,  $T$ , and  $\sigma$ , as indicated in Cor. 3.

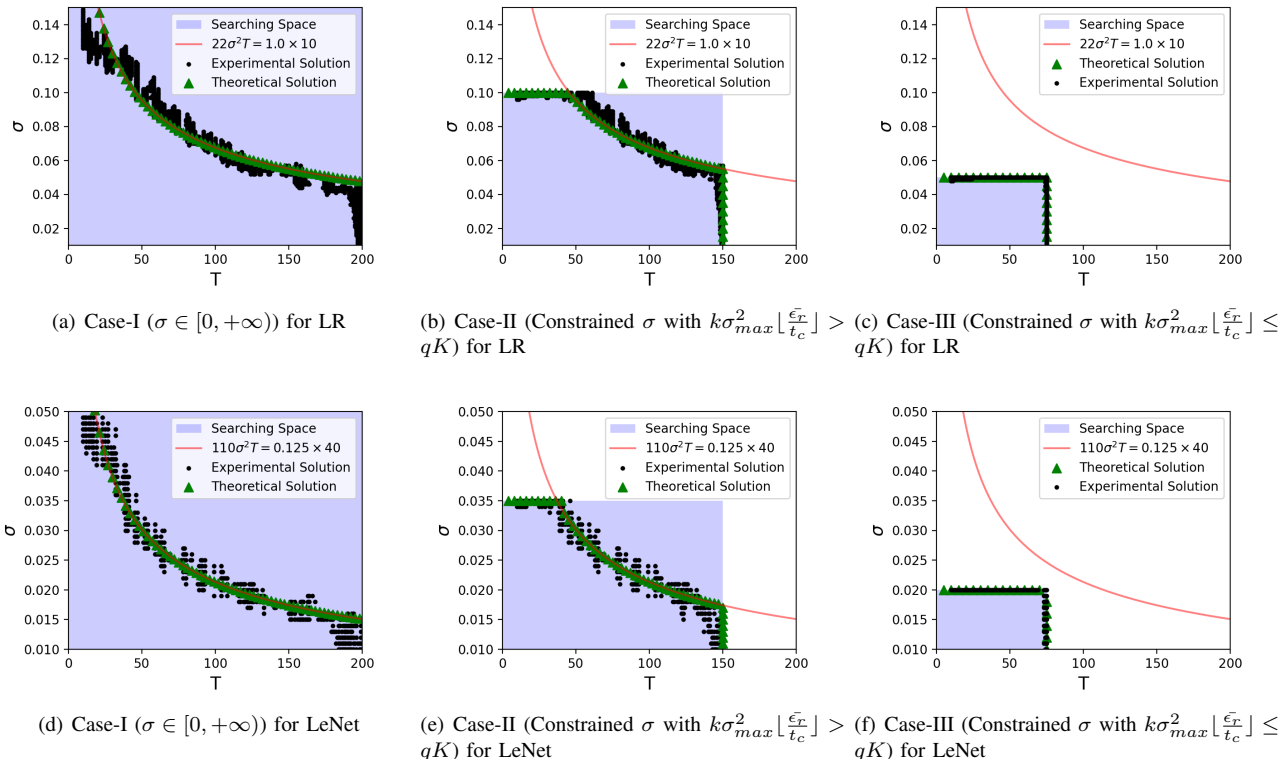


Fig. 3. **Pareto solution for LR and LeNet model with different searching space.** With total  $K = 10$ ,  $q = 1.0$  and  $E = 20$  in LR model, Fig. 3(a) shows the Pareto solution in Case-I where we assume  $\sigma \in [0.01, 0.15]$  and  $T \in [1, \dots, 200]$  with  $\lfloor \frac{\epsilon_r}{t_c} \rfloor = 200$ . Fig. 3(b) shows the Pareto solution in the Case-II as  $k\sigma_{max}^2 \lfloor \frac{\epsilon_r}{t_c} \rfloor > qK$  where  $\lfloor \frac{\epsilon_r}{t_c} \rfloor = 150$  and  $\sigma_{max} = 0.10$ . Fig. 3(c) shows the Pareto solution in Case-III as  $k\sigma_{max}^2 \lfloor \frac{\epsilon_r}{t_c} \rfloor \leq qK$  where  $\lfloor \frac{\epsilon_r}{t_c} \rfloor = 75$  and  $\sigma_{max} = 0.50$ . With total  $K = 40$ ,  $q = 0.125$  and  $E = 20$  in LR model, Fig. 3(d) shows the Pareto solution in Case-I where we assume  $\sigma \in [0.01, 0.05]$  and  $T \in [1, \dots, 200]$  with  $\lfloor \frac{\epsilon_r}{t_c} \rfloor = 200$ . Fig. 3(e) shows the Pareto solution in the wide range case as  $k\sigma_{max}^2 \lfloor \frac{\epsilon_r}{t_c} \rfloor > qK$  where  $\lfloor \frac{\epsilon_r}{t_c} \rfloor = 150$  and  $\sigma_{max} = 0.035$ . Fig. 3(f) shows the Pareto solution in the small range case as  $k\sigma_{max}^2 \lfloor \frac{\epsilon_r}{t_c} \rfloor \leq qK$  where  $\lfloor \frac{\epsilon_r}{t_c} \rfloor = 75$  and  $\sigma_{max} = 0.02$ .

leakage.

Table II show the time to get the optimal parameter design with given  $T$  and  $q$  from server. For our proposed method, the process of guiding parameter design can be divided into two parts: 1) The pre-experiment time denoted as  $t_0$  is much smaller than the formal training time since the public dataset using in pre-experiment is much smaller; 2) The main training time is global training epoch  $T_r$  since the clients directly calculate the optimal  $\sigma$  with given  $q_r$  and  $T_r$  according to Theorem 3. For the method **Training with Budget** and **Training Until Convergence**, they needs to search the optimal  $\sigma$ , thus, its computation complexity is  $\Theta(n_\sigma T_r)$ , where  $n_\sigma$  is the number of different  $\sigma$ .

Similarly, Table III contrasts the time required to locate the entire Pareto set under different methods. It reveals that our proposed method reduces the search time by  $n_q$  times compared to the two methods, **Training with Budget** and **Training Until Convergence**, i.e., it eliminates the need to search over  $q$ . This efficiency is attributed to Theorem 2, which aids in determining the sample ratio  $q$  given  $\sigma$  and  $T$ .

## VI. CONCLUSION AND DISCUSSION

Bearing in mind the aim of achieving optimal privacy-utility trade-off within an acceptable training efficiency constraint,

TABLE II  
COMPLEXITY COMPARISON (GUIDING PARAMETER DESIGN)

Method	Computational Complexity
Our Method	$t_0 + \Theta(T_r)$
Training with Budget [16], [17]	$\Theta(n_\sigma T_r)$
Training until Convergence [5], [18]	$\Theta(n_\sigma T_r)$

TABLE III  
TABLE OF COMPLEXITY COMPARISON (ACHIEVING PARETO SET)

Method	Computational Complexity
Our Method	$t_0 + \Theta(n_\sigma T_r)$
Training with Budget [16], [17]	$\Theta(n_q n_\sigma T_r)$
Training until Convergence [5], [18]	$\Theta(n_q n_\sigma T_r)$

we formulate the constrained bi-objective optimization formulation in Differential Privacy Federated Learning (DPFL). The theoretical analysis of the constrained bi-objective optimization problem can serve as an important guidance of the parameter design in DPFL, which could help us get rid of the expensive neural network training and federated system evaluation [7], [30], [48]. By using a small proportion of public data, we can get an approximate estimation of the exact relationship among  $T$ ,  $\sigma$ , and  $q$ .

In future, we can also do similar theoretical analysis for

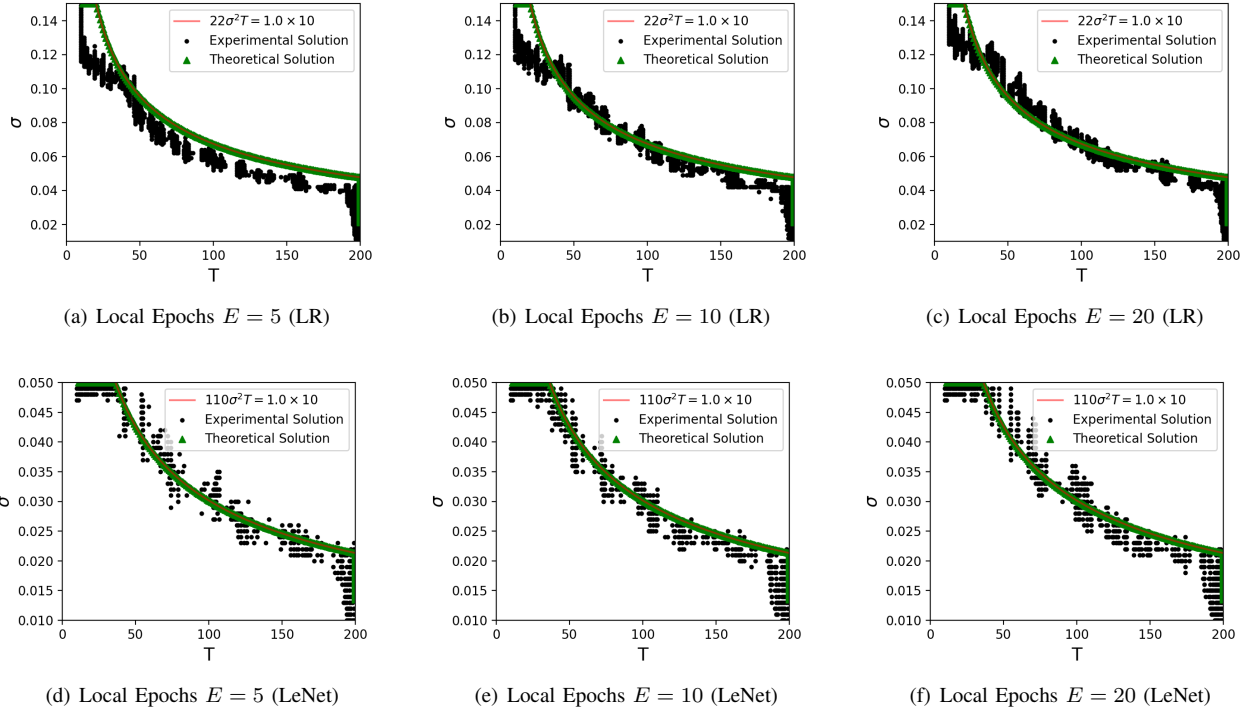


Fig. 4. **Pareto solutions for LR and LeNet with different local epochs.** With  $K = 10$  and  $q = 1.0$ , Fig 4(a), 4(b), and 4(c) show the Pareto solution for LR with local epochs  $E = 5, 10, 20$  respectively. With  $K = 10$  and  $q = 1.0$ , Fig 4(d), 4(e), and 4(f) show the Pareto solution for LeNet with local epochs  $E = 5, 10, 20$  respectively.

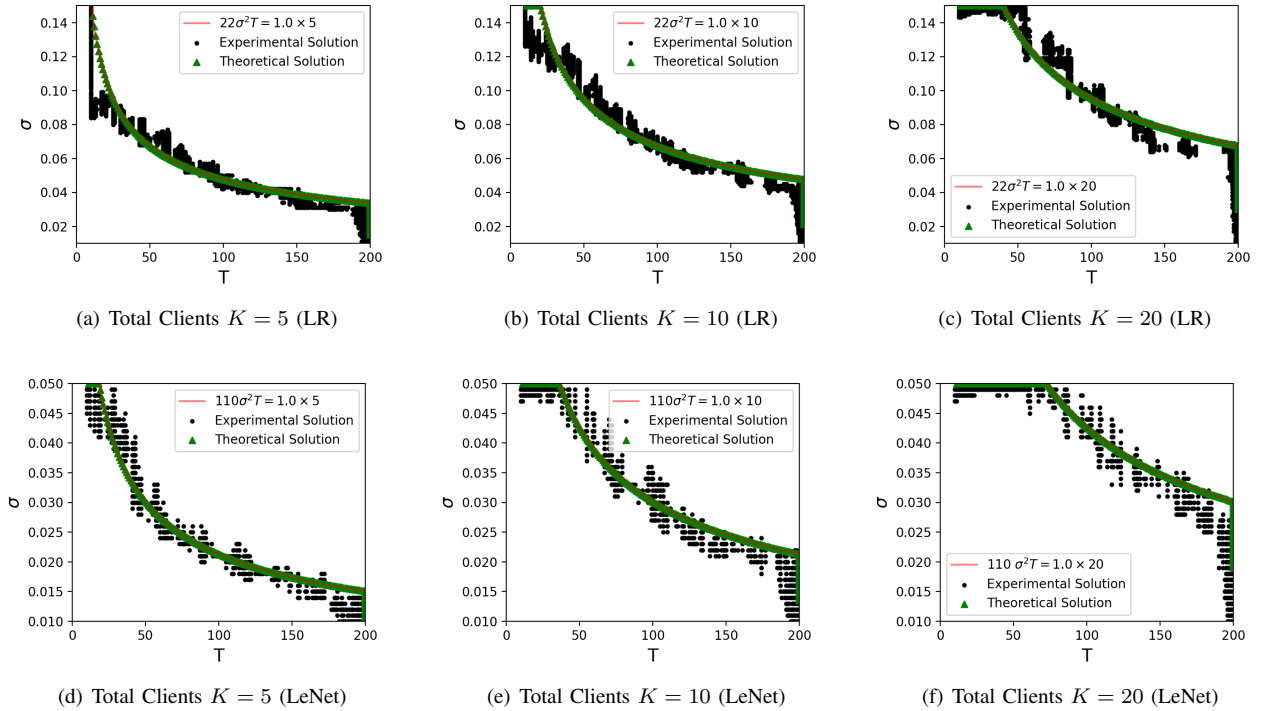


Fig. 5. **Pareto solutions for LR and LeNet with different number of total clients.** With  $q = 1.0$  and  $E = 20$ , Fig. 5(a), 5(b), 5(c) show the Pareto solution for LR with number of total clients  $K = 5, 10, 20$  respectively. With  $q = 1.0$  and  $E = 20$ , Fig. 5(d), 5(e), 5(f) show the Pareto solution for LeNet with number of total clients  $K = 5, 10, 20$  respectively.

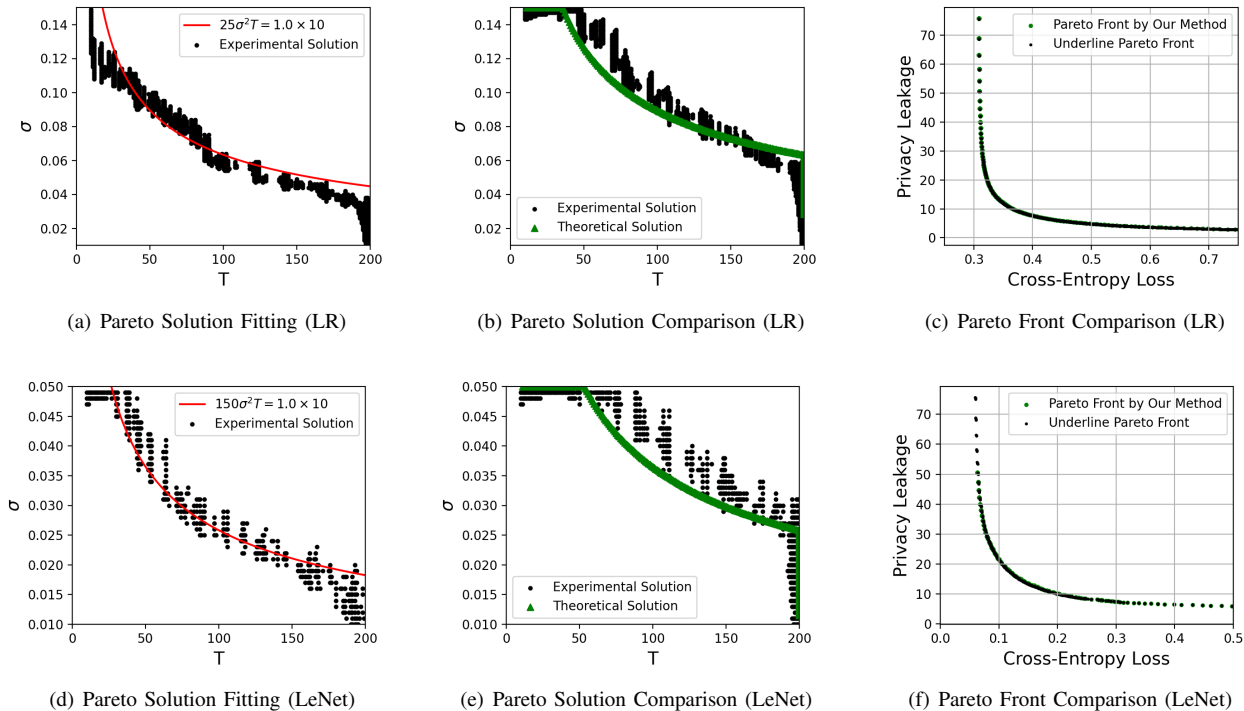


Fig. 6. **Parameter Design Guidance by Public Dataset.** With  $K = 10$  and  $q = 1.0$ , Fig. 6(a) shows the Pareto solution on public dataset and the solutions are fitted by the line  $25\sigma^2T = 1.0 \times 10$ . Fig. 6(b) compares the derived theoretical Pareto solution from public dataset and the underline experimental Pareto solution of case  $K = 40$  and  $q = 0.5$ . Fig. 6(c) compares the derived theoretical Pareto front from public dataset and the underline experimental Pareto front of case  $K = 40$  and  $q = 0.5$ . With  $K = 10$  and  $q = 1.0$ , Fig. 6(d) shows the Pareto solution on public dataset and the solutions are fitted by the line  $150\sigma^2T = 1.0 \times 10$ . Fig. 6(e) compares the derived theoretical Pareto solution from public dataset and the underline experimental Pareto solution of case  $K = 40$  and  $q = 0.5$ . Fig. 6(f) compares the derived theoretical Pareto front from public dataset and the underline experimental Pareto front of case  $K = 40$  and  $q = 0.5$ .

different protection mechanisms in the federated learning framework, as long as it has or could be given a good enough upper-bound of utility loss.

## REFERENCES

- [1] H. B. McMahan, E. Moore, D. Ramage, S. Hampson, and B. A. y Arcas, "Communication-Efficient Learning of Deep Networks from Decentralized Data," in *Artificial intelligence and statistics*. PMLR, 2017, pp. 1273–1282.
- [2] Q. Yang, Y. Liu, Y. Cheng, Y. Kang, T. Chen, and H. Yu, "Federated Learning," *Synthesis Lectures on Artificial Intelligence and Machine Learning*, vol. 13, no. 3, pp. 1–207, Dec. 2019.
- [3] C. Dwork, A. Roth et al., "The algorithmic foundations of differential privacy," *Foundations and Trends® in Theoretical Computer Science*, vol. 9, no. 3–4, pp. 211–407, 2014.
- [4] M. Abadi, A. Chu, I. Goodfellow, H. B. McMahan, I. Mironov, K. Talwar, and L. Zhang, "Deep learning with differential privacy," in *Proceedings of the 2016 ACM SIGSAC Conference on Computer and Communications Security*, ser. CCS '16. New York, NY, USA: Association for Computing Machinery, 2016, p. 308–318. [Online]. Available: <https://doi.org/10.1145/2976749.2978318>
- [5] Q. Yang, Y. Liu, T. Chen, and Y. Tong, "Federated machine learning: Concept and applications," *ACM Transactions on Intelligent Systems and Technology (TIST)*, vol. 10, no. 2, pp. 1–19, 2019.
- [6] X. Zhang, H. Gu, L. Fan, K. Chen, and Q. Yang, "No free lunch theorem for security and utility in federated learning," *ACM Trans. Intell. Syst. Technol.*, vol. 14, no. 1, nov 2022. [Online]. Available: <https://doi.org/10.1145/3563219>
- [7] Y. Kang, H. Gu, X. Tang, Y. He, Y. Zhang, J. He, Y. Han, L. Fan, and Q. Yang, "Optimizing privacy, utility and efficiency in constrained multi-objective federated learning," *arXiv preprint arXiv:2305.00312*, 2023.
- [8] Z. He, T. Zhang, and R. B. Lee, "Model inversion attacks against collaborative inference," in *Proceedings of the 35th Annual Computer Security Applications Conference*, 2019, pp. 148–162.
- [9] L. Zhu, Z. Liu, and S. Han, "Deep leakage from gradients," *Advances in neural information processing systems*, vol. 32, 2019.
- [10] J. Geiping, H. Bauermeister, H. Dröge, and M. Moeller, "Inverting gradients-how easy is it to break privacy in federated learning?" *Advances in Neural Information Processing Systems*, vol. 33, pp. 16 937–16 947, 2020.
- [11] H. Yin, A. Mallya, A. Vahdat, J. M. Alvarez, J. Kautz, and P. Molchanov, "See through gradients: Image batch recovery via gradinversion," in *Proceedings of the IEEE/CVF Conference on Computer Vision and Pattern Recognition*, 2021, pp. 16 337–16 346.
- [12] B. Zhao, K. R. Mopuri, and H. Bilen, "idlg: Improved deep leakage from gradients," *arXiv preprint arXiv:2001.02610*, 2020.
- [13] J. Konečný, H. B. McMahan, F. X. Yu, P. Richtárik, A. T. Suresh, and D. Bacon, "Federated learning: Strategies for improving communication efficiency," *arXiv preprint arXiv:1610.05492*, 2016.
- [14] A. Singh, P. Vepakomma, O. Gupta, and R. Raskar, "Detailed comparison of communication efficiency of split learning and federated learning," *arXiv preprint arXiv:1909.09145*, 2019.
- [15] A. Ghosh, J. Chung, D. Yin, and K. Ramchandran, "An efficient framework for clustered federated learning," *Advances in Neural Information Processing Systems*, vol. 33, pp. 19 586–19 597, 2020.
- [16] R. C. Geyer, T. Klein, and M. Nabi, "Differentially private federated learning: A client level perspective," *arXiv preprint arXiv:1712.07557*, 2017.
- [17] K. Wei, J. Li, M. Ding, C. Ma, H. H. Yang, F. Farokhi, S. Jin, T. Q. Quek, and H. V. Poor, "Federated learning with differential privacy: Algorithms and performance analysis," *IEEE Transactions on Information Forensics and Security*, vol. 15, pp. 3454–3469, 2020.
- [18] H. Wu, C. Chen, and L. Wang, "A theoretical perspective on differentially private federated multi-task learning," *arXiv preprint arXiv:2011.07179*, 2020.
- [19] Y. Fraboni, R. Vidal, L. Kameni, and M. Lorenzi, "On the impact of client sampling on federated learning convergence," 2022. [Online]. Available: [https://openreview.net/forum?id=edN\\_G\\_4njyi](https://openreview.net/forum?id=edN_G_4njyi)
- [20] Y. J. Cho, J. Wang, and G. Joshi, "Client selection in federated learning:

- Convergence analysis and power-of-choice selection strategies,” *arXiv preprint arXiv:2010.01243*, 2020.
- [21] C. Dwork, F. McSherry, K. Nissim, and A. Smith, “Calibrating noise to sensitivity in private data analysis,” in *Theory of Cryptography: Third Theory of Cryptography Conference, TCC 2006, New York, NY, USA, March 4-7, 2006, Proceedings 3*. Springer, 2006, pp. 265–284.
- [22] C. Dwork and M. Naor, “On the difficulties of disclosure prevention in statistical databases or the case for differential privacy,” *Journal of Privacy and Confidentiality*, vol. 2, no. 1, 2010.
- [23] C. Dwork, “Differential privacy,” in *International colloquium on automata, languages, and programming*. Springer, 2006, pp. 1–12.
- [24] Z. Bu, J. Dong, Q. Long, and W. J. Su, “Deep learning with gaussian differential privacy,” *Harvard data science review*, vol. 2020, no. 23, pp. 10–1162, 2020.
- [25] I. Mironov, “Rényi differential privacy,” in *2017 IEEE 30th computer security foundations symposium (CSF)*. IEEE, 2017, pp. 263–275.
- [26] M. Seif, R. Tandon, and M. Li, “Wireless federated learning with local differential privacy,” in *2020 IEEE International Symposium on Information Theory (ISIT)*. IEEE, 2020, pp. 2604–2609.
- [27] S. Truex, L. Liu, K.-H. Chow, M. E. Gursoy, and W. Wei, “Ldp-fed: Federated learning with local differential privacy,” in *Proceedings of the Third ACM International Workshop on Edge Systems, Analytics and Networking*, 2020, pp. 61–66.
- [28] M. Ehrgott, *Multicriteria optimization*. Springer Science & Business Media, 2005, vol. 491.
- [29] N. Gunantara, “A review of multi-objective optimization: Methods and its applications,” *Cogent Engineering*, vol. 5, no. 1, p. 1502242, 2018.
- [30] K. Deb, A. Pratap, S. Agarwal, and T. Meyarivan, “A fast and elitist multiobjective genetic algorithm: Nsga-ii,” *IEEE transactions on evolutionary computation*, vol. 6, no. 2, pp. 182–197, 2002.
- [31] K. Deb and H. Jain, “An evolutionary many-objective optimization algorithm using reference-point-based nondominated sorting approach, part i: Solving problems with box constraints,” *IEEE Transactions on Evolutionary Computation*, vol. 18, no. 4, pp. 577–601, 2014.
- [32] M. Kim, T. Hiroyasu, M. Miki, and S. Watanabe, “Spea2+: Improving the performance of the strength pareto evolutionary algorithm 2,” in *Parallel Problem Solving from Nature-PPSN VIII: 8th International Conference, Birmingham, UK, September 18-22, 2004, Proceedings 8*. Springer, 2004, pp. 742–751.
- [33] Q. Zhang and H. Li, “Moea/d: A multiobjective evolutionary algorithm based on decomposition,” *IEEE Transactions on evolutionary computation*, vol. 11, no. 6, pp. 712–731, 2007.
- [34] A. Biswas, C. Fuentes, and C. Hoyle, “A multi-objective bayesian optimization approach using the weighted tchebycheff method,” *Journal of mechanical design*, vol. 144, no. 1, p. 011703, 2022.
- [35] S. Daulton, D. Eriksson, M. Balandat, and E. Bakshy, “Multi-objective bayesian optimization over high-dimensional search spaces,” in *Uncertainty in Artificial Intelligence*. PMLR, 2022, pp. 507–517.
- [36] M. Laumanns and J. Ocenasek, “Bayesian optimization algorithms for multi-objective optimization,” in *International Conference on Parallel Problem Solving from Nature*. Springer, 2002, pp. 298–307.
- [37] K. Yang, M. Emmerich, A. Deutz, and T. Bäck, “Multi-objective bayesian global optimization using expected hypervolume improvement gradient,” *Swarm and evolutionary computation*, vol. 44, pp. 945–956, 2019.
- [38] J.-A. Désidéri, “Mgda variants for multi-objective optimization,” Ph.D. dissertation, INRIA, 2012.
- [39] —, “Multiple-gradient descent algorithm (mgda) for multiobjective optimization,” *Comptes Rendus Mathématique*, vol. 350, no. 5-6, pp. 313–318, 2012.
- [40] X. Liu, X. Tong, and Q. Liu, “Profiling pareto front with multi-objective stein variational gradient descent,” *Advances in Neural Information Processing Systems*, vol. 34, pp. 14 721–14 733, 2021.
- [41] S. Liu and L. N. Vicente, “The stochastic multi-gradient algorithm for multi-objective optimization and its application to supervised machine learning,” *Annals of Operations Research*, pp. 1–30, 2021.
- [42] D. Mahapatra and V. Rajan, “Multi-task learning with user preferences: Gradient descent with controlled ascent in pareto optimization,” in *International Conference on Machine Learning*. PMLR, 2020, pp. 6597–6607.
- [43] X. Zhang, X. Chen, M. Hong, Z. S. Wu, and J. Yi, “Understanding clipping for federated learning: Convergence and client-level differential privacy,” in *International Conference on Machine Learning, ICML 2022, 2022*.
- [44] Y. Lecun, L. Bottou, Y. Bengio, and P. Haffner, “Gradient-based learning applied to document recognition,” *Proceedings of the IEEE*, vol. 86, no. 11, pp. 2278–2324, 1998.
- [45] L. Deng, “The mnist database of handwritten digit images for machine learning research,” *IEEE Signal Processing Magazine*, vol. 29, no. 6, pp. 141–142, 2012.
- [46] K. He, X. Zhang, S. Ren, and J. Sun, “Deep residual learning for image recognition,” in *Proceedings of the IEEE conference on computer vision and pattern recognition*, 2016, pp. 770–778.
- [47] A. Krizhevsky, G. Hinton et al., “Learning multiple layers of features from tiny images,” 2009.
- [48] X. Lin, Z. Yang, X. Zhang, and Q. Zhang, “Pareto set learning for expensive multi-objective optimization,” *Advances in Neural Information Processing Systems*, vol. 35, pp. 19 231–19 247, 2022.